# Evaluation and prediction of the behavior of the Beauharnois dam, using FLAC3D

Davide Lamberti, Emanuele Catalano, Riccardo Stucchi Lombardi Engineering Ltd., Giubiasco, Switzerland

ABSTRACT: The paper presents a study carried out to analyze the behavior of a concrete power station affected by AAR, the Beauharnois power plant. A step-by-step method is proposed to integrate the physics aspects affecting the swelling reaction, in particular: reaction kinetics, temperature field and degree of saturation. The calibration of the numerical model is performed on the basis of the displacement measurements that are available at three different measuring points. The calibrated model is furtherly used to provide a prediction of the future dam behavior in the next 50 years. This calculation exercise was proposed in the frame of the 16th International Benchmark Workshop on Numerical Analysis of Dams.

#### 1 INTRODUCTION

The Theme B of the 16th International Benchmark Workshop on Numerical Analysis of Dams concerns the numerical modelling of the alkali-aggregate reaction (AAR) in the Beauharnois Dam (only the single power unit 12 with its two neighboring units will be considered, see Figure 1).

Due to the complexity of AAR, a step-by-step method is adopted, characterized by the progressive introduction of the different parameters influencing the swelling reaction: the development of the chemical reaction, the influence of temperature, and the influence of humidity. The objective of the analysis is to reproduce the observed behavior of the dam and to estimate the progress for the next 50 years.

The paper presents the main aspects of the numerical model that was prepared, the swelling model that was chosen to reproduce the behavior of the AAR reaction and its results. Some comments on the general behavior of the dam are also presented.

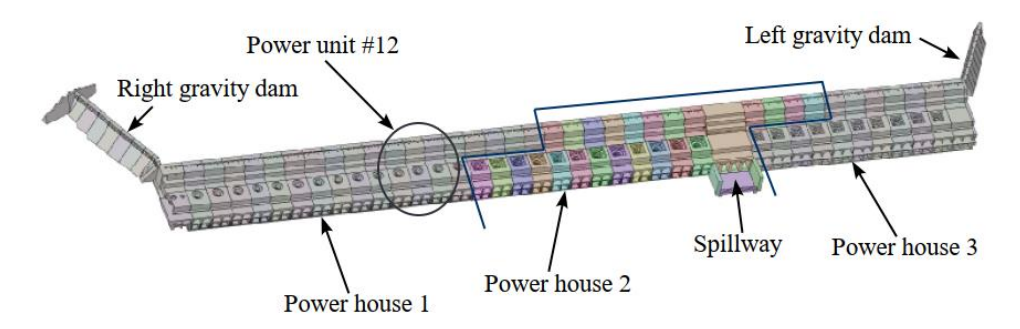


Figure 1: Beauharnois Dam, with position of the Power unit 12 (Benchmark formulation document, 2021).

# 2 AAR MODEL

The proposed AAR model includes four of the main known factors affecting the magnitude and spatial distribution of the AAR-induced concrete expansion: the reaction kinetics, the temperature effects, the dependency on the stress state and the influence of humidity.

The dependency of the structure stiffness on the progression of the alkali-aggregate reaction is not included in the model.

#### 2.1 Reaction kinetics

The AAR expansion model adopted is based on the work of Capra & Bournazel 1998. This model assumes that AAR follows a first-order kinetic law, described by:

$$\frac{dA}{dt} = k \cdot (1 - A) \tag{1}$$

where A represents the percentage of alkali that have reacted and measures the advancement of the reaction varying between 0 and 1; k is the kinetic constant, i.e., the reaction velocity at time t = 0 (hence A = 0).

In addition, the model assumes that the chemical reaction and the concrete expansion are dissociated: the concrete expansion starts occurring only when the cracks, which are initially generated within the aggregates, also propagate in the cement paste. To dissociate the reaction and the expansion, a parameter  $A_0$  is defined. When the reaction advance exceeds  $A_0$ , the macroscopically observable expansive phenomenon begins. The link between the AAR induced concrete

expansion ( $\varepsilon_{AAR}$ ) and the reaction advance (A) is therefore defined by the following bi-linear law (Figure 2).

$$\varepsilon_{AAR} = \begin{cases} 0 & \text{se } A < A_0 \\ \frac{A - A_0}{1 - A_0} \cdot \varepsilon_{\infty} & \text{se } A > A_0 \end{cases}$$
 (2)

where  $\varepsilon_{\infty}$  is the AAR induced concrete expansion at infinite time.

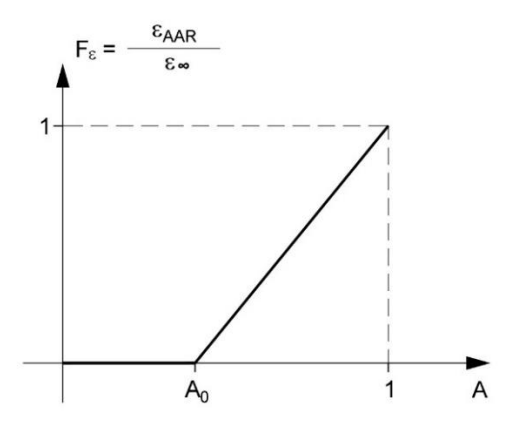


Figure 2: Relationship between normalized expansion ( $\varepsilon_{AAR}/\varepsilon_{\infty}$ ) and reaction advancement (A).

#### 2.2 Temperature

For all chemical reactions, temperature causes a change in the reaction velocity. In the considered model, the temperature influences the kinetic constant (k) of the chemical reaction according to the Arrhenius equation:

$$k = k_0 \cdot e^{\frac{E_a}{R} \cdot \left(\frac{1}{\theta_0} - \frac{1}{\theta}\right)} \tag{3}$$

where  $k_0$  = reaction rate at the reference temperature  $\theta_0$ ;  $E_a$  = activation energy, a typical activation energy of 45 kJ/mol is used for the alkali-aggregate reaction (Gimal et al., 2010; Morenon et al., 2021); R = gas constant (8.31 J/mol/K);  $\theta$  = temperature at which the reaction rate k is to be determined (temperatures are in Kelvin degrees).

According to Arrhenius' law, the relationship between temperature and reaction rate is nonlinear, characterized by a doubling of the reaction rate every  $10^{\circ}$ C for an activation energy  $E_a$  of 45 kJ/mol.

## 2.3 Stress state

It is known that the stress state within a concrete structure influences the AAR induced expansion. A compressive state of stress limits the expansion. To account for the effect of the stress state on the development of the reaction, reference is made to the formulation proposed by Saouma & Perotti, 2006. According to this approach, weights varying between 0 and 1 are assigned to each principal direction depending on the stress state. The higher the compression in a direction, the lower is the weight assigned to that direction. When the compression reaches a value of  $\sigma_u$ , the swelling in that direction is totally inhibited. Figure 3 shows some examples of weight assignment.

In all possible combinations, the sum of the weights is always equal to 1, meaning that the expansion is redistributed in the three principal directions keeping the volumetric expansion constant, as shown in experimental studies by Multon & Toutlemonde, 2006.

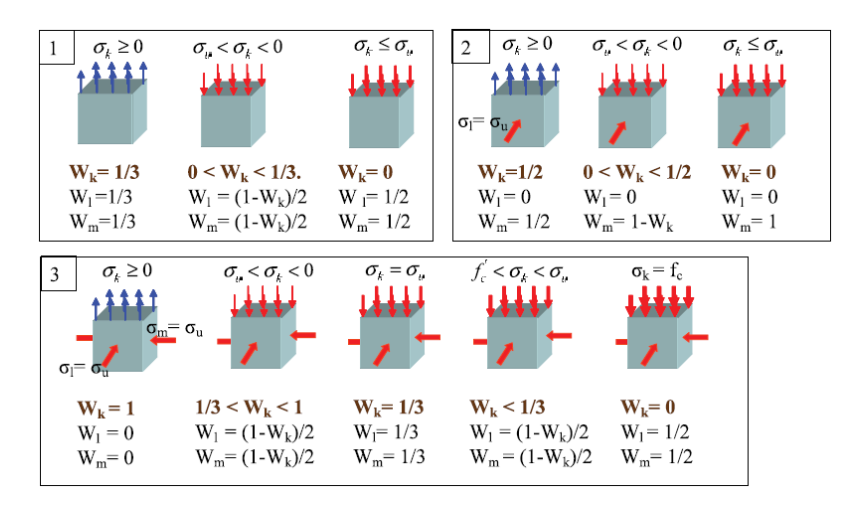


Figure 3: Weights for the redistribution of volumetric expansion (Saouma & Perotti 2006).

#### 2.4 Humidity

Humidity plays an important role in determining the AAR. Since AAR needs water to occur, a low humidity hinders the development of the reaction. The most relevant parameter for considering the effect of the humidity on the AAR is the saturation ratio ( $S_r$ ) inside the structure. The model proposed by Poyet et al., 2004 considers a coupling between the saturation ratio and the reaction kinetics by introducing two parameters:

$$\frac{dA}{dt} = k \cdot \alpha \cdot (\beta - A) \tag{4}$$

where  $\alpha$  modifies the velocity of the reaction; and  $\beta$  modifies the maximum reaction advancement.

Based on several laboratory tests Poyet et al., 2004 conclude that the relationship between the two parameters and the saturation ratio is linear with  $\alpha = \beta = S_r$ .

#### 3 MONITORING DATA

The construction of the dam took place in three phases between 1932 and 1961. The dam is equipped with a topographic auscultation system since 1973. Measurements of displacements in the y-direction (upstream-downstream, positive if towards downstream) and z-direction (vertical direction, positive if upwards) at three different points were available. The behavior of the dam in the first 40 years is not recorded. The measured values will therefore refer to relative and not to total displacements. The three points are defined according to their position: *Crest* at the top of the dam, *Turbine pit* located in the turbine chamber and *Turbine floor* located further downstream. The position of the three points is represented in Figure 4. The measured displacements that were available for model calibration are represented in Figure 5.

No other information was available, that could be useful in the interpretation of the behavior of the structure, such as laboratory tests, crack pattern in the structure, stress measurements, direct expansion measurement within the structure by means of extensometers.

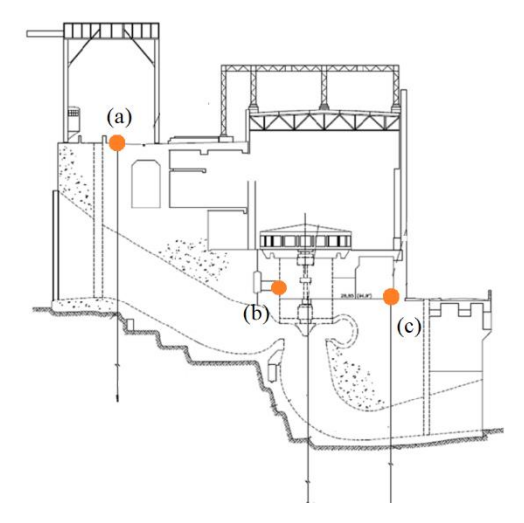


Figure 4: position of the three points: Crest (a), Turbine pit (b) and Turbine floor (c) (Benchmark formulation document, 2021).

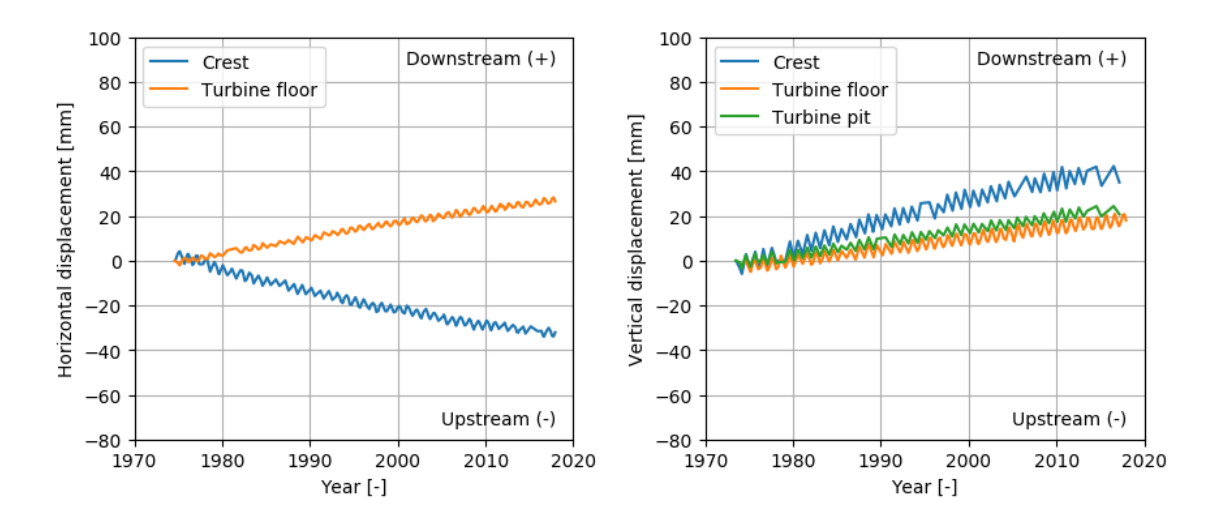


Figure 5: Topographic displacements for the three points (period 1974-2018).

## 4 NUMERICAL MODEL

# 4.1 Geometry

The numerical analyses proposed in this paper were carried out using FLAC3D vers. 7.0 (Itasca Consulting Group Inc. 2016), which implements the finite-difference method (FDM) and allows performing mechanical analyses in the linear and nonlinear domains. The model reproduces the geometry of three power units (11 to 13) including the foundation. The water intake part has a height of approximately 21.5 m and includes the penstocks, the upstream gates and the busbar. The power plant is approximately 24 m high and includes the generator unit, the scroll case, the draft tube, the tailrace and the downstream gates. A cold joint separates the water intake part from the power plant. The mesh (Figure 6) is composed mainly of hexahedral elements with a size of approximately 1 m for the dam body, while the foundation is formed by a coarser mesh with variable size from 1 to 20 m.

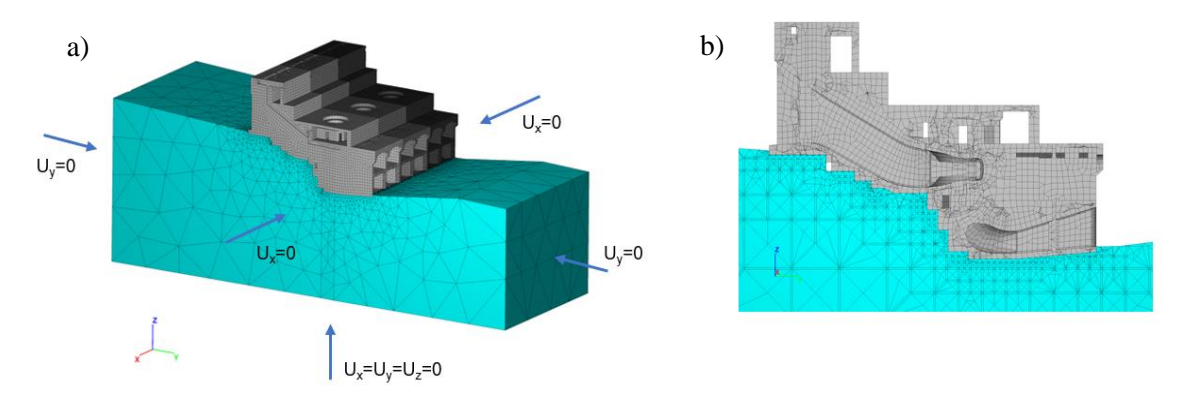


Figure 6: (a) Three-dimensional view of dam-rock system with displacement boundary conditions, (b) Finite element mesh of the Power unit 12, longitudinal section (y-z plane) (Benchmark formulation document, 2021).

## 4.2 Interfaces

The interfaces between the water intake part and the power plant, or between the different power units, have been modelled whit a non-linear behavior (except for static linear elastic analysis where the connection is bonded). The interfaces between the rock and the power unit have been kept bonded. Table 1 shows the main interface parameters introduced in the numerical model.

Table 1: Interfaces parameters.

Properties	Interfaces	Interfaces
	rock/concrete	concrete/concrete
Shear stiffness [kPa/m]	1.0E+08	1.0E+08
Normal stiffness [kPa/m]	1.0E+08	1.0E+08
Cohesion [kPa]	elastic	3.0E+02
Tensile strength [kPa]	elastic	1.0E+01
Friction angle [°]	elastic	45

## 4.3 Material properties

Linear elastic behavior was assumed for the concrete and the foundation materials. Physical and mechanical properties are listed in Table 2. It is important to note that thermo-mechanical effects are not considered in the analysis, since a nil coefficient of thermal expansion is assumed.

All creep and relaxation influence on the stress state induced by AAR strains are neglected. Also, any computation of crack initiation was not performed. The presence of reinforcements within the structure is neglected.

Table 2: Material properties.

Properties	Concrete	Foundation
Density [t/m <sup>3</sup> ]	2.36	2.62
Poisson's ratio [-]	0.21	0.20
Young Modulus [GPa]	26	-
Deformation Modulus [GPa)]	-	30
Specific heat [J/ kg °C]	917	800
Thermal conductivity [W/ m °C]	2.9	4.3
Coef. of thermal expansion [°C <sup>-1</sup> ]	0	0
Reference temperature [°C]	10	4

# 4.4 Boundary conditions

For determining the thermal state within the structure, the thermal boundary conditions shown in Figure 7 have been applied to the model. Temperatures at boundaries were available on a daily average basis, and it was assumed that these temperatures can be repeated each year. Hygral boundary conditions, necessary to calculate the saturation within the model, have been provided by the formulators in the form of capillary pressure and relative humidity as shown in Figure 8.

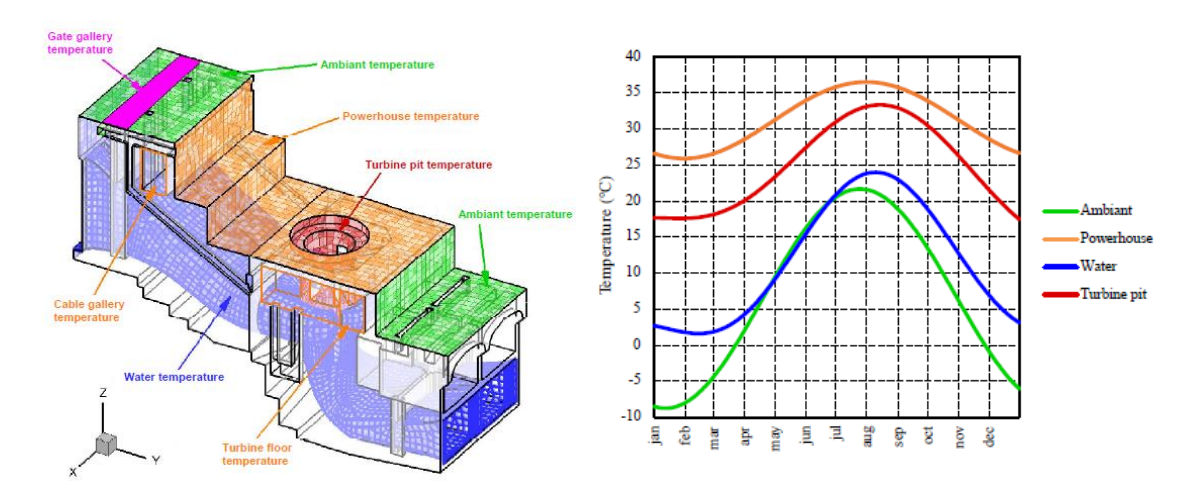


Figure 7: Thermal boundary conditions (Benchmark formulation document, 2021).

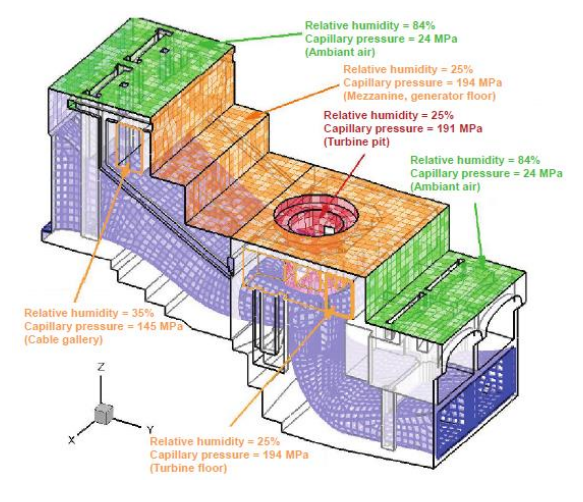


Figure 8: Hygral boundary conditions (Benchmark formulation document, 2021).

## 5 CALCULATION STEPS

# 5.1 Introduction

The simulation of the AAR effects in a structure is a complex task, because of the number of parameters influencing the swelling reaction. For this reason, a step-by-step procedure is implemented by progressively introducing each parameter of the model.

The steps listed in Table 3 are performed.

Table 3: Performed calculations.

Task	Stress redistribution	Thermal effects	Hygral effects
0 (calibration)	-	-	-
A	X	-	-
В	X	X	-
C	X	X	X

For the tasks A to C it is required to compute the stress field within the structure. The loading conditions considered in the analyses account for:

- Gravity loads;
- Hydrostatic water pressure. The hydrostatic load computation assumes an upstream water level at 46.10 m and a downstream water level at 21.4 m;
- Induced load caused by the concrete expansion.

In order to properly reproduce the effects of the seasonal temperature variation within one year, calculations are carried out with a 1-month timestep, starting in 1932 until 2017 (calibration period). The prediction of the model is computed until 2067 to consider a prediction period of 50 years.

# 5.2 Task 0: First calibration of the AAR model

In the lack of specific laboratory tests on concrete, a calibration of the numerical model has been performed to fit the field measurements. The two parameters that must be calibrated are:

- $\varepsilon_{\infty} = AAR$  induced concrete expansion at infinite time
- $k_0$  = reaction rate at the reference temperature  $\theta_0$

The method of thermal analogy was used to estimate the initial parameters of the AAR model. This method consists in linking a thermal expansion to the volumetric deformation given by the swelling due to the alkali-aggregate reaction. Assuming an isotropic distribution of the expansion induced the AAR (no redistribution based on stress state), a constant temperature field equal to the reference temperature (no thermal effects), and neglecting the hygral effects, a one-year computation of the displacements induced by the AAR reaction is enough to obtain the evolution of displacements over the desired period.

The calibration of the model is performed by minimizing the difference between the measured displacements and the displacements obtained by the model in the calibration period (1974-2018).

## 5.3 Task A: Constant temperature, fully saturated

The effect of the chemical reaction is computed by adopting a constant and uniform temperature of 10 degrees (equal to the reference temperature, no thermal effects then). Also, the concrete is considered as completely saturated. The effect of the stress state is accounted for in this task.

#### 5.4 Task B: Introduction of thermal effects

In a second stage of simulation, the effect of temperature on the development of the reaction is introduced.

Based on the temperature boundary conditions, which consist of daily temperature measurements over a year, a thermal conductivity analysis is performed. After 7 years all transient effects were found to be negligible. The thermal state in the dam is known at any moment during the year after this procedure.

However, for simplicity, the choice was made to compute an equivalent temperature for each point in the dam, to be kept constant over the entire period of simulation of the AAR reaction propagation. The equivalent temperature is defined as the temperature for which the total progress

of the AAR reaction is the same as the one computed considering the daily variation of the temperature. The equivalent temperature was computed as the temperature that satisfy this condition over a period of 100 years. The final thermal field that was computed is represented in Figure 9. It is worth noting that the equivalent temperature is higher than the yearly average temperature, since the expansion increase due to the temperatures above the average exceeds the expansion reduction due to the temperatures below the average, because of the non-linearity of the expansion-temperature relationship.

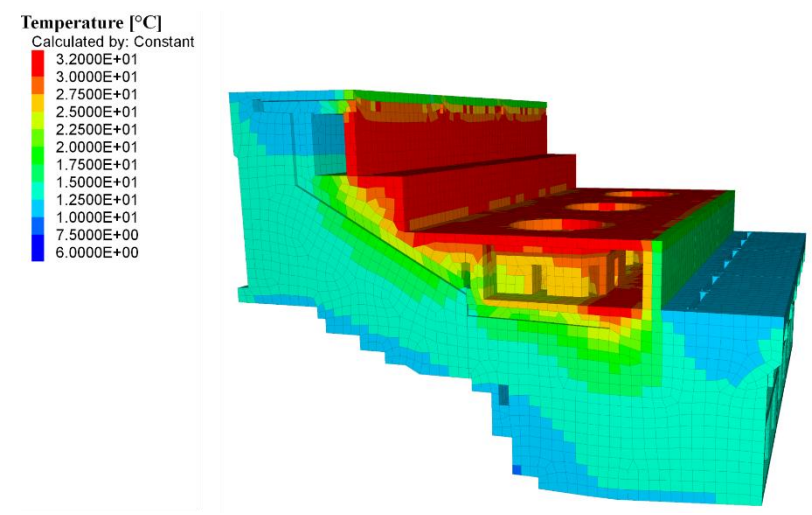


Figure 9: Equivalent temperature distribution used for calculation.

# 5.5 Task C: Introduction of hygral effects

The last case studied includes the effects generated by humidity. As described in section 2.4, humidity plays an important role in determining the AAR. Since AAR needs water to occur, a low humidity hinders the development of the reaction. The most relevant parameter for considering the effect of the humidity on the AAR is the saturation ratio  $(S_r)$  inside the structure.

To compute a saturation distribution inside the power plant, the software FEFLOW vers. 7.3 (Diersch 2014) was used, adopting the Mualem model (Van Genuchten 1980) with the following parameters: a = 18.6 MPa and m = 0.44.

The distribution of saturation that was computed (Figure 10) has been considered constant over the entire calculation period.

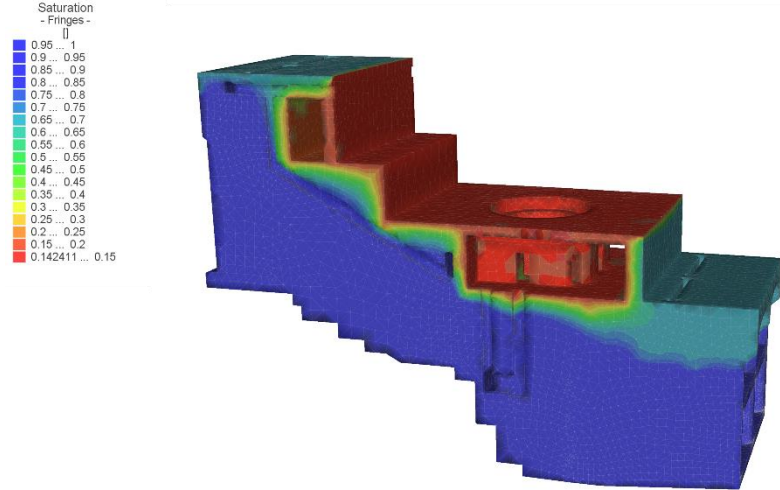


Figure 10: Saturation ratio  $(S_r)$  in the power unit 12.

## 6 RESULTS AND DISCUSSION

# 6.1 Displacement induced by the AAR expansion

The results of the model in terms of displacements of the monitored points, are shown in Figure 12 for the period 1940-2067. The calibrated set of parameters for the AAR model are listed in Table 4 for the four calibration steps. The parameter  $A_{\theta}$  was not calibrated but was defined in order to reproduce a latency time, i.e., a period without concrete expansion after the chemical reaction start, of approximately 10-15 years.

The results obtained by considering only the reaction kinetics (Task 0) are remarkably satisfactory. The time evolution of the displacements is well reproduced for all the monitored points. A little overestimation is obtained for the horizontal displacement of the *Crest* and for the vertical displacement of the *Turbine Floor*, while a little overestimation is obtained for the vertical displacement of the *Crest* and for the horizontal displacement of the *Turbine Floor*. The concrete expansion at infinite time obtained by the calibration is 3900 µm/m, which seems to be plausible if compared with other structures (Amberg et al, 2013). The value is kept constant for the other tasks

The introduction of the effect of the stress state (Task A) and of the temperature (Task B) produce minor changes in the predicted displacements, except for the vertical displacement of the Turbine Floor, which is overestimated by the model in the calibration period. This is supposed to be the result of the swelling redistribution due to the stress state. The concrete expansion in the x-direction is hindered by the presence of the adjacent blocks, leading to higher compressive stress in that direction that cause a redistribution of the expansion in the other less-compressed directions. The same effect, though minor, is visible also in the predicted vertical displacements for the *Crest* and the *Turbine Pit*.

The best agreement between the measured displacements and the predicted ones is obtained with the introduction of the effect of the saturation (Task C). The displacements of all the points are correctly reproduced by the model, except the vertical displacement of the Turbine Floor. It has to be noted that the best result in the calibration process was obtained by neglecting the effect of the saturation ratio on the final advance of the reaction. Therefore, the parameter  $\beta$  has been taken equal to 1.

The good superposition of the curves for most of the points, indicates that, the proposed model provides a correct description of the AAR phenomenon. However, the increase of complexity in the model does not produce substantial improvements in the approximation of the curves. On the basis of the limited information available regarding the behavior of the dam, the introduction of other effects than the reaction kinetics seems not justifiable. A more comprehensive understanding of the behavior of the dam supported by stress measurements, crack pattern layout or direct measurement of the concrete expansion would be needed, in the opinion of the authors, to support the introduction of further elements and complexity in the model.

The prediction for the next 50 years, indicates that the displacement velocity would decrease in the future without, however, reaching a full stabilization phase in the next 50 years. This is compatible with field observations for other structures in which the full stabilization phase is not yet observed. The deceleration visible in the displacement is compatible with the reaction advance predicted by the model. Figure 11 shows, for the Task C, that the reaction level in most of the dam has already reached a level of more than 80-90 per cent, in particular in the regions with higher temperatures. The zones with a lower reaction level are located in the less saturated zones.

Table 4: AAR model parameters.

Parameters	Task 0	Task A	Task B	Task C
$\varepsilon_{\infty}$ [ $\mu$ m/m]	3.9E+03	3.9E+03	3.9E+03	3.9E+03
$k_0$ [1/day]	4.1E-05	4.1E-05	4.1E-05	6.0E-05
$\theta_0$ [°C]	10°C	10°C	10°C	10°C
$E_a$ [kJ/mol]	-	-	45	45
$A_0$ [-]	2.0 E-02	2.0 E-02	2.0 E-02	2.0 E-02
α[-]	-	-	-	$S_r$
$\beta$ [-]	-	-	-	1
$\sigma_u$ [MPa]	-	10	10	10

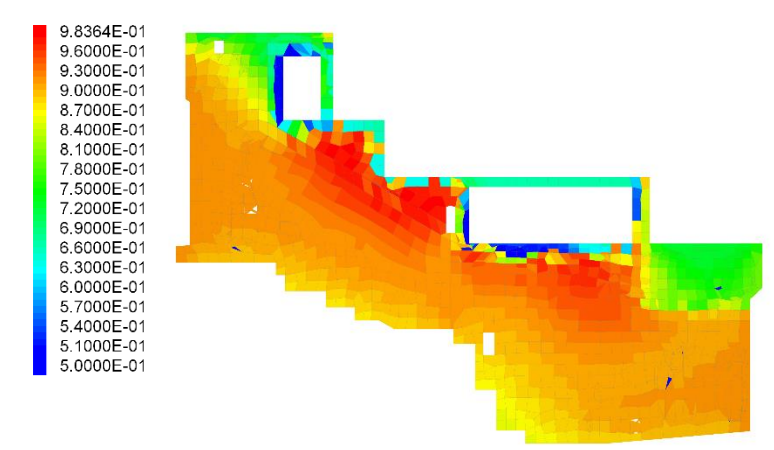


Figure 11: Level of reaction (A) in 2017, which represent the advancement of the reaction.

## 6.2 Stresses induced by the AAR expansion

Concrete expansion produces stresses in the structure. Stresses that were computed over the surfaces represented in Figure 13 are presented in this section. Figure 14 shows the evolution of the average stress (i.e., resultant force divided by the area) in the previously defined surfaces for the period 1937-2067. For the calculation of the average stresses, the resultants acting on the unit 12 are considered. For the Intake/Unit surface, the resultants acting on the intake are considered.

A relevant compressive stress develops in the X direction. The compressive stress in the X direction reaches 10 MPa in 2067, which is the value that inhibits the expansion according to the adopted model. A compression develops also in the Y direction, reaching 8 MPa in the Intake/Unit surface, caused by the concrete expansion restrained by the rock foundation. The compressive force is transmitted to the rock by means of a sort of compressed arch. In fact, a positive Z stress and a negative Y stress is obtained for the Rock/Unit surface. The ratio between the shear (Y) and normal (Z) stress is about 1.6, which could possibly lead to a slip at the concrete/rock interface.

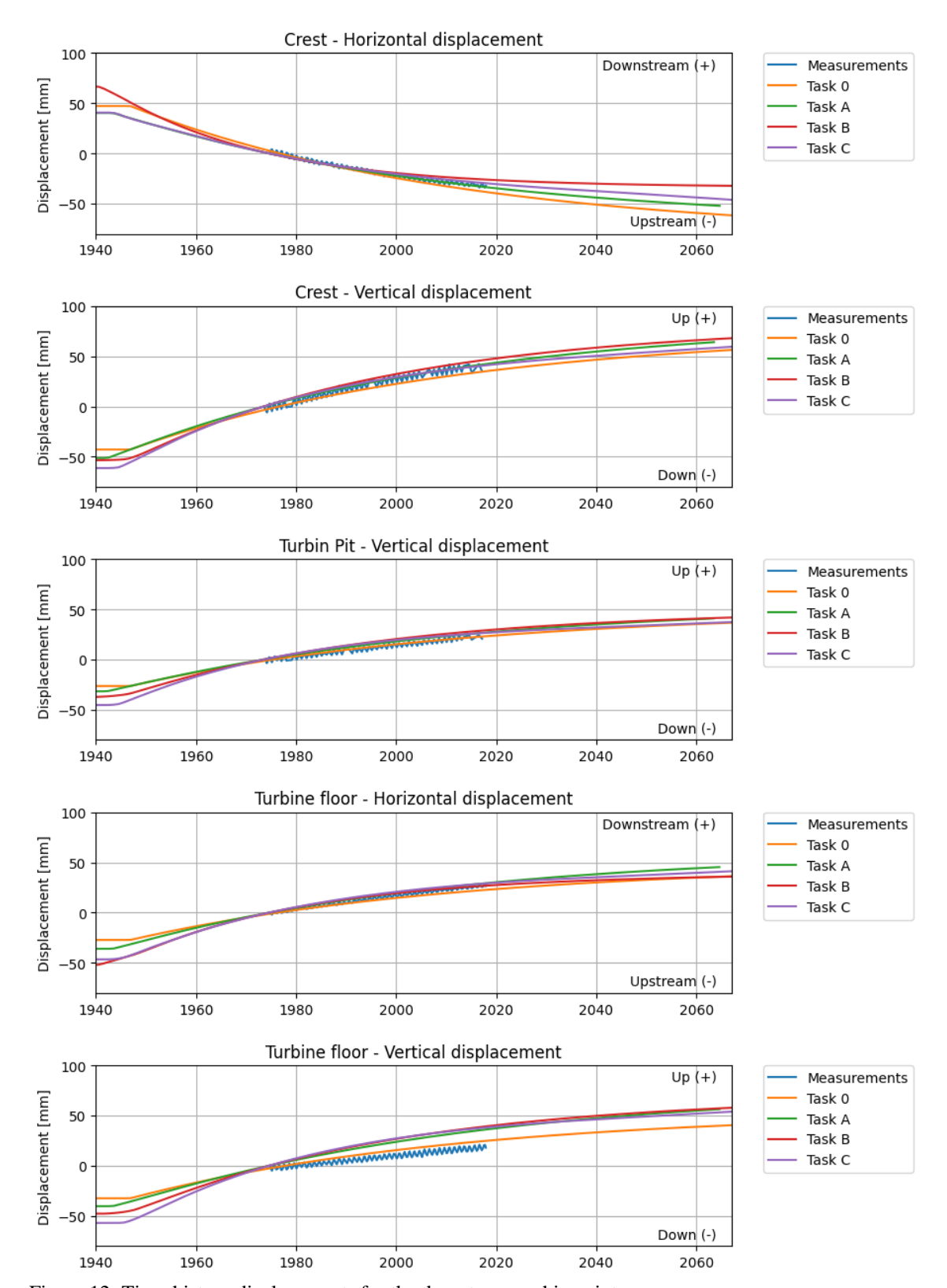


Figure 12: Time-history displacements for the three topographic points

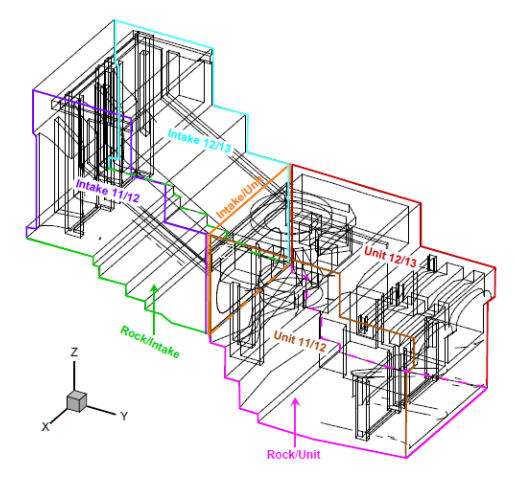


Figure 13: Definition of the surfaces in the model (Benchmark formulation document, 2021).

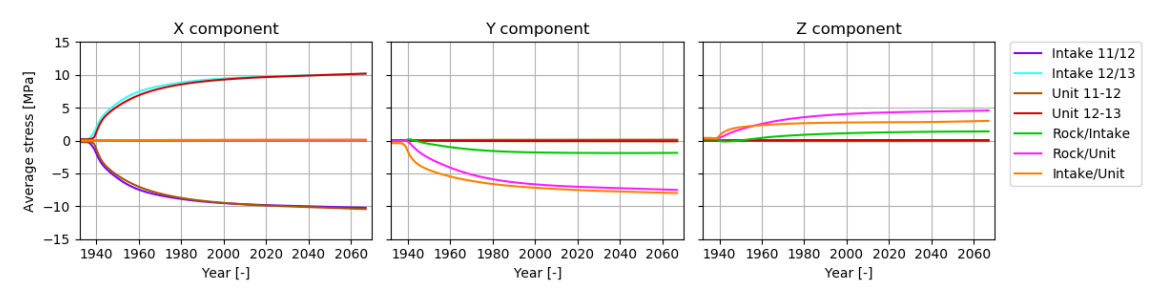


Figure 14: Average stress in the interfaces for the Task C.

## 7 CONCLUSIONS

The behavior of the Beauharnois Dam affected by AAR is evaluated by means of a numerical model accounting for the effects of the reaction kinetics, of the temperature, of the stress state and of the humidity. This calculation exercise was proposed in the frame of the 16th International Benchmark Workshop on Numerical Analysis of Dams.

The model is calibrated on the measured displacement in 5 points in the dam in the period 1974-2018. A prediction for the next 50 years is also performed. The best agreement between the model and the measurements is obtained by including in the model all the above listed effects. However, a remarkable satisfactory result is also achieved by considering the reaction kinetics only. In other words, the addition of complexity in the model does not produce substantial improvements in the approximation of the actual behavior. A more comprehensive understanding of the actual behavior of the dam in terms of stress state (in situ stress test, crack pattern layout) and expansion distribution (by means of direct expansion measurements) would be needed, in the opinion of the authors, for supporting the introduction in a reliable way of further effects in the model.

Some general conclusions regarding the behavior of the dam can be drawn from the results of the model. A compressive stress state arises in the X direction, its magnitude being affected by the assumptions of the model, though. Also, in the upstream-downstream direction compressive stress develop, which are transferred to the rock foundation by relevant shear stresses, which could lead to slippages in the rock-concrete interface.

As stated before, these general considerations must be supported by further data for defining properly a possible rehabilitation work. According to the obtained dam behavior, a possible intervention can be the realization of vertical slot cuts between units (YZ plane) and between intakes

and units (XZ plane) in order to relief the compressive stress in the X direction and in the Y direction, respectively.

#### REFERENCES

- Amberg, F., Stucchi, R., Brizzo, N. 2013. The effect of temperature on the development of the Alkali Aggregate Reaction at the Pian Telessio dam. 9th ICOLD European Club Symposium, Venice
- Benchmark formulation document, Roth S.-N., Miquel B., *Theme B: AAR affected dam. Evaluation and prediction of the behavior of the Beauharnois dam*, 16th International Benchmark Workshop on Numerical analysis of Dams, 2021.
- Bérubé, M.-A., Frenette, J., Pedneault, A., Rivest, M. 2002. *Laboratory assessment of the potential rate of ASR expansion of field concrete*. Cement, Concrete and Aggregates, Vol. 24, n. 1, pp. 13-19
- Capra B., Bournazel J.P. 1998. Modeling of induced mechanical effects of alkali-aggregate reactions. Cement and concrete Research, 2251-260.
- Diersch H-J. 2014. FEFLOW, Finite Element Modeling of Flow, Mass and Heat Transport in Porous and Fractured Media, Springer-Verlag Berlin Heidelberg, Germany.
- Grimal E., Sellier A., Multon S., La Pape Y., Bourdarot E. 2010. *Concrete Concrete modelling for expertise of structures affected by alkali aggregate reaction*. Cement and Concrete Research, 502–507.
- Itasca Consulting Group, Inc. 2016. FLAC Fast Lagrangian Analysis of Continua, Ver. 8.0. Minneapolis.
  Morenon P., Sellier A., Multon S., Grimal E., Kolmayer P. 2021. Benchmark Study Results: EdF/LMDC.
  In: Saouma V.E. (eds) Diagnosis & Prognosis of AAR Affected Structures. RILEM State-of-the-Art Reports, vol 31. Springer.
- Multon, S., Toutlemonde, F. 2006. *Effect of applied stresses on alkali-silica reaction-induced expansions*. Cement and Concrete Research 36 912-920.
- Poyet, S., Sellier, A., Capra, B., Foray, G., Torrenti, J.-M., Cognon, H., Bourdarot, E. 2004. *Modelling of Alkali-Silica Reaction in Concrete, Part 2: Influence of Water on ASR*, Proc. Of the 12th Int. Conf. on Alkali-Aggregate Reaction in Concrete, Beijing, China.
- 2021. 16th International Benchmark Workshop on Numerical Analysis of Dams, Theme B, *Evaluation, and prediction of the behavior of the Beauharnois dam*. Ljubljana, Slovenia.
- Saouma V., Perotti, L. 2006. *Constitutive Model for Alkali-Aggregate Reactions*. ACI Materials Journal 103(3) 194-202
- M. Th. van Genuchten 1980 A closed-form equation for predicting the hydraulic conductivity of unsaturated soils. Soil Science Society of America Journal 44.5, pp.892–898.